European Journal of Pharmaceutics and Biopharmaceutics 76 (2010) 514–524

Contents lists available at ScienceDirect

European Journal of Pharmaceutics and Biopharmaceutics

journal homepage: www.elsevier.com/locate/ejpb

Research paper

Spectral analysis of doxorubicin accumulation and the indirect quantification of its DNA intercalation

Ondřej Hovorka [a,*], Vladimír Šubr [b], David Větvička [a], Lubomír Kovář [a], Jiří Strohalm [b], Martin Strohalm [a], Aleš Benda [c], Martin Hof [c], Karel Ulbrich [b], Blanka Říhová [a]

[a] Institute of Microbiology, Academy of Sciences of the Czech Republic, Prague, Czech Republic
[b] Institute of Macromolecular Chemistry, Academy of Sciences of the Czech Republic, Prague, Czech Republic
[c] J. Heyrovsky Institute of Physical Chemistry, Academy of Sciences of the Czech Republic, Prague, Czech Republic

ARTICLE INFO

Article history:
Received 29 January 2010
Accepted in revised form 12 July 2010
Available online 16 July 2010

Keywords:
Doxorubicin
Fluorescence
FLIM
Drug delivery
HPMA copolymers

ABSTRACT

There is a wide range of techniques utilizing fluorescence of doxorubicin (Dox) commonly used for analysis of intracellular accumulation and destiny of various drug delivery systems containing this anthracycline antibiotic. Unfortunately, results of these studies can be significantly influenced by doxorubicin degradation product, 7,8-dehydro-9,10-desacetyldoxorubicinone (D*) forming spontaneously in aqueous environment, whose fluorescence strongly interfere with that of doxorubicin. Here, we define two microscopy techniques enabling to distinguish and separate Dox and D* emission based either on its spectral properties or on fluorescence lifetime analysis. To analyze influx and nuclear accumulation of Dox (free or polymer-bound) by flow cytometry, we propose using an indirect method based on its DNA intercalation competition with Hoechst 33342 rather than a direct measurement of doxorubicin fluorescence inside the cells.

1. Introduction

Doxorubicin (Dox) is a cytostatic drug of first choice in many malignancies [1]. Its high efficacy in cancer treatment is restrained by its unwanted side-effects – it causes serious damage to normal proliferating cells, including hematopoietic stem cells in bone marrow, gastrointestinal mucosal cells, and gonad cells; however, its cardiotoxicity seems to be the limiting factor in most cases [2]. To eliminate such complications, a large effort is spent to design new drug delivery systems (DDS) with optimized pharmacokinetics and pharmacodynamics and eventually targeted to tumor sites [3–5]. Macromolecular systems based on linear polymers [6], polymeric micelles [7], nanoparticles [8], liposomes [9], dendrimeres [10], and many other systems have been designed up to now as potential Dox carriers. However, until now, a few drug delivery systems have entered clinical trials and even less have proceeded through – ex. liposomal preparation of doxorubicin, commercially known as Caelix. One of the widely studied polymer carrier-based DDS, which has begun clinical trials in the late 1990s, was Dox bound to a *N*-(2-hydroxypropyl)methacrylamide (HPMA) copolymer through a proteolytically cleavable oligopeptidic GlyPheLeuGly spacer, also known as PK1 (FCE 28 068) [11]. Also, its antibody-conjugated analogue has undergone clinical evaluation in the treatment of human breast cancer [4,12].

To improve the design of such systems, detailed study of the intracellular pathway, the rate of accumulation inside cells, and the intracellular translocation of active compounds to target compartments is quite necessary. For such studies, an intrinsic fluorescence of Dox seemed to be a great tool. Unfortunately, the situation is much more complicated than it might seem to be at first glance. It has been documented that doxorubicin fluorescence is dependent on the environment – it has a lower fluorescence yield in aqueous media, when compared to the hydrophobic environment in lipidic structures like membranes and/or after binding to macromolecular carrier systems. Moreover, the intensity of Dox fluorescence significantly decreases after intercalation into DNA, where it gives 30–40 times lower fluorescence yield when compared to a non-intercalated drug [13,14]. Therefore, quantification or visualization of plain fluorescence gives a rather marginal and very complicated set of signals, which must be carefully analyzed to avoid misinterpretation of data. The situation is further complicated by the existence of the doxorubicin degradation byproduct, the highly hydrophobic 7,8-dehydro-9,10-desacetyldoxorubicinone (D*), described by Fiallo et al. [13], which regularly spontaneously

Abbreviations: Dox, doxorubicin; D*, 7,8-dehydro-9,10-desacetyldoxorubicinone; FLIM, fluorescence lifetime imaging; HPMA, *N*-(2-Hydroxypropyl)methacrylamide; AOBS, Acousto-Optical Beam Splitter; SPAD, Single-Photon Avalanche Diode; TTTR mode, time-tagged time-resolved mode; TCSPC, time-correlated single photon counting.

* Corresponding author. MBU AV CR, Vídeňská 1083, 142 20, Prague 4, Czech Republic. Tel.: +420 2 41062756; fax: +420 2 41061143.
E-mail address: hovorka@biomed.cas.cz (O. Hovorka).

0939-6411/$ - see front matter © 2010 Elsevier B.V. All rights reserved.
doi:10.1016/j.ejpb.2010.07.008

originates from free or even covalently bound Dox in aqueous media and whose fluorescence yield is about 30 times stronger compared to the parent drug. Due to this enormous fluorescent activity, the degradation byproduct almost completely overlaps original Dox fluorescence. Unfortunately, the source of possible misinterpretation does not consist only of a different intensity of fluorescence of both compounds, but also of their different physicochemical behavior, namely the tendency towards hydrophobic interactions, e.g., with cell membranes, etc.

Here, we analyze *in vitro* intracellular spectra emitted by free or polymer-bound Dox to separate Dox from D* fluorescence. We also propose a new technique, which enables the analysis of doxorubicin accumulation in nuclear DNA indirectly by flow cytometry.

2. Materials and methods

2.1. Synthesis of conjugates

2.1.1. Materials

1-Aminopropan-2-ol, methacryloyl chloride, glycylglycine (Gly-Gly), glycyl-L-phenylalanine (GlyPhe), L-leucylglycine (LeuGly), 2,2′-azobis(isobutyronitrile) (AIBN), *N*,*N*-dimethylformamide (DMF), 4-(dimethylamino)pyridine, *N*,*N*′-dicyclohexylcarbodiimide (DCC), 4,5-dihydrothiazole-2-thiol, tetrahydrofurane (THF) dimethyl sulfoxide (DMSO), and triethylamine (Et_3N) were purchased from Sigma–Aldrich, Czech Republic. Doxorubicin hydrochloride (Dox·HCl) was purchased from Meiji Seika Kaisha, Japan. Amino derivate of DY-615 (DY-615-NH_2) was purchased from Dyomics, Germany.

2.1.2. Synthesis and characterization of monomers

N-(2-Hydroxypropyl)methacrylamide (HPMA) was synthesized by the reaction of methacryloyl chloride with 1-aminopropan-2-ol in dichloromethane in the presence of sodium carbonate, as described previously [15].

N-Methacryloylglycylglycine 4-nitrophenyl ester (Ma-GlyGly-ONp) was prepared by the reaction of *N*-methacryloylglycylglycine with 4-nitrophenol in DMF in the presence of DCC [16]. *N*-Methacryloylglycyl-D,L-phenylalanylleucylglycine 4-nitrophenyl ester (Ma-Gly-D,L-PheLeuGly-ONp) was prepared by the reaction of *N*-methacryloylglycyl-D,L-phenylalanylleucylglycine with 4-nitrophenol in THF in the presence of DCC [17].

N-Methacryloylglycyl-D,L-phenylalanylleucylglycyldoxorubicin (Ma-Gly-D,L-PheLeuGly-Dox) was prepared by the reaction of Ma-Gly-D,L-PheLeuGly-ONp with doxorubicin hydrochloride in DMF at 4 °C in the presence of Et_3N [15].

3-(*N*-Methacryloylglycylglycyl)thiazolidine-2-thione (Ma-Gly-Gly-TT) was prepared by the reaction of *N*-methacryloylglycylglycine with 4,5-dihydrothiazole-2-thiol in DMF in the presence of DCC and a catalytic amount of DMAP, as described earlier [18].

Monomers were characterized by melting point, elemental analysis, ^1H NMR, and HPLC [16].

2.1.3. Synthesis of polymer precursors

Polymer precursors **1** poly(HPMA-*co*-Ma-GlyGly-ONp) and **2** poly(HPMA-*co*-Ma-Gly-D,L-PheLeuGly-ONp), containing 4-nitrophenoxy (ONp) reactive groups, were prepared by precipitation radical copolymerization in acetone for 24 h at 50 °C [19].

Polymer precursor **3** poly(HPMA-*co*-Ma-Gly-D,L-PheLeuGly-DOX-*co*-Ma-GlyGly-TT), containing carbonylthiazolidine-2-thione (TT) reactive groups, was prepared by the solution radical copolymerization of HPMA (0.150 g, 1.05 mmol) Ma-Gly-D,L-PheLeuGly-Dox (0.033 g, 3.34×10^{-2} mmol) and Ma-GlyGly-TT (0.010 g, 3.34×10^{-2} mmol) in DMSO for 6 h at 60 °C [16]. The concentration of monomers was 12.5 wt%, and the concentration of the initiator AIBN was 1 wt% in a polymerization mixture.

2.1.4. Synthesis of polymer-Dox conjugates

Polymer conjugates **4** poly(HPMA-*co*-Ma-GlyGly-Dox) and **5** poly(HPMA-*co*-Ma-Gly-D,L-PheLeuGly-Dox) were prepared by the reaction of polymer precursors **1** or **2** with Dox·HCl in DMSO in the presence of Et_3N [17,18].

Polymer conjugate **6** poly(HPMA-*co*-Ma-Gly-D,L-PheLeuGly-Dox-*co*-Ma-GlyGly-DY-615) was prepared by the reaction of polymer precursor **3** (0.05 g, 7.5×10^{-3} mmol TT groups) with an amine derivate of DY-615 (0.003 g, 4.6 μmol) in DMSO (0.5 mL) in the presence of Et_3N (1 μL, 4.6 μmol) for 2 h at room temperature. TT reactive groups remaining in the copolymer after the reaction were aminolyzed by the addition of 1-amino-2-propanol (1 μL), and the polymer conjugate was isolated by precipitation into an acetone/diethyl ether mixture (3:1), filtered off, and dried in vacuum.

To remove unbound Dox, fluorescent dye DY-615, and the Dox degradation byproduct D* from polymer conjugates **4**–**6**, the polymer conjugates were dissolved in methanol and subjected to repeated gel filtration chromatography on a Sephadex LH-20 with methanol as eluent.

2.1.5. Characterization of polymer precursors and conjugates

Polymer precursors **1**–**3** and polymer conjugates **4**–**6** were characterized by average molecular weight M_w, polydispersity M_w/M_n, and content of reactive groups (TT, ONp), doxorubicin, and fluorescent dye (DY-615).

Determination of molecular weight and polymer polydispersity was carried out on a HPLC Shimadzu system equipped with UV, Optilab® rEX differential refractometer, and multiangle light scattering DAWN® 8™ (Wyatt Technology, CA, USA) detectors using a 0.3 M acetate buffer (CH_3COONa/CH_3COOH; pH 6.5; 0.5 g/L NaN_3) and a Superose™ 6 column.

The content of carbonylthiazolidine-2-thione (TT), 4-nitrophenoxy (ONp) groups, doxorubicin, and DY-615 in polymers was determined spectrophotometrically on a Specord 205 (Analytik Jena, Germany) using molar absorption coefficient for TT groups ε_{305} = 10,700 L mol^{-1} cm^{-1} (methanol), for ONp ε_{274} = 9800 L mol^{-1} cm^{-1} (DMSO), for Dox ε_{484} = 10,300 L mol^{-1} cm^{-1} (methanol), and for DY-615 ε_{621} = 200,000 (ethanol). The characteristics of final polymer conjugates **4**–**6** are summarized in Table 1.

Verification of the purity of polymer conjugates **4**–**6**, specifically the absence of the Dox degradation byproduct D*, was carried out by HPLC on a SGX C18 reverse phase column (Tessek, Czech Republic) equipped with a fluoroMonitor™ 4100 fluorescence detector (LDC Analytical, FL, USA; Ex = 484 nm, Em = 560 nm). A water/acetonitrile gradient elution (0–100% acetonitrile) was used. Flow rate was 1 mL/min.

Table 1
Characteristics of polymer conjugates.

Polymer conjugate	Spacer	M_w	M_w/M_n	Dox content wt%	DY-615 content mol%
4	GlyGly-Dox	21,200	1.61	9.7	–
5	Gly-D,L-PheLeuGly-Dox	47,300	1.60	8.0	–
6	Gly-D,L-PheLeuGly-Dox GlyGly-DY-615	40,500	1.77	7.0	0.7

2.1.6. Preparation and characterization of 7,8-dehydro-9,10-desacetyldoxorubicinone (D)*

Polymer conjugate **5** poly(HPMA-*co*-Ma-Gly-D,L-PheLeuGly-Dox) (0.5 g) was incubated in a phosphate buffer (50 mL) of pH 7.4 for 4 days at 37 °C in the absence of light.

Water was evaporated, and the oily residue was diluted with methanol and again evaporated. The residue was finally dissolved in methanol (30 mL), and the solution was separated from precipitated buffer salts and subjected to chromatography on a Sephadex LH-20 with methanol as eluent. The last violet fraction was collected; methanol was evaporated to an oily residue, which was precipitated by the addition of diethyl ether. The yield of D* was 5 mg. The purity and structure of the D* was confirmed by HPLC on a SGX C18 reverse phase column (Tessek) equipped with a fluorescence detector (Ex = 484 nm and Em = 560 nm; single peak at 25.57 min). Mass spectra were acquired using a 9.4T APEX™ Ultra FTICR (Fourier Transform Ion Cyclotron Resonance) mass spectrometer equipped with an Apollo II dual ion source (Bruker Daltonics, MA, USA). The sample was measured in negative ion mode using the NALDI™ ionization technique (Nano-Assisted Laser Desorption/Ionization) (Bruker Daltonics) and a 355 nm Nd:Yag laser. The peak $[M-H]^-$ 335.0561 was the most intense in the spectrum. The structure of 7,8-dehydro-9,10-desacetyldoxorubicinone is shown in Fig. 1A. Comparison of the UV–VIS spectra of doxorubicin hydrochloride with its degradation byproduct D* in methanol is shown in Fig. 1B.

2.2. Cells

2.2.1. 3T3 mouse fibrosarcoma

3T3 cells (ATCC: CCL-92) were grown in cultivation flasks at 37 °C with 5% CO_2 in Dulbecco's modified Eagle's medium (Gibco Laboratories, MA, USA) without phenol red, with 4 mM L-glutamine (Gibco), adjusted to contain 1.5 g/L sodium bicarbonate and 4.5 g/L glucose, fetal calf serum 10% v/v, 100 U/mL penicillin, and 100 mg/mL streptomycin.

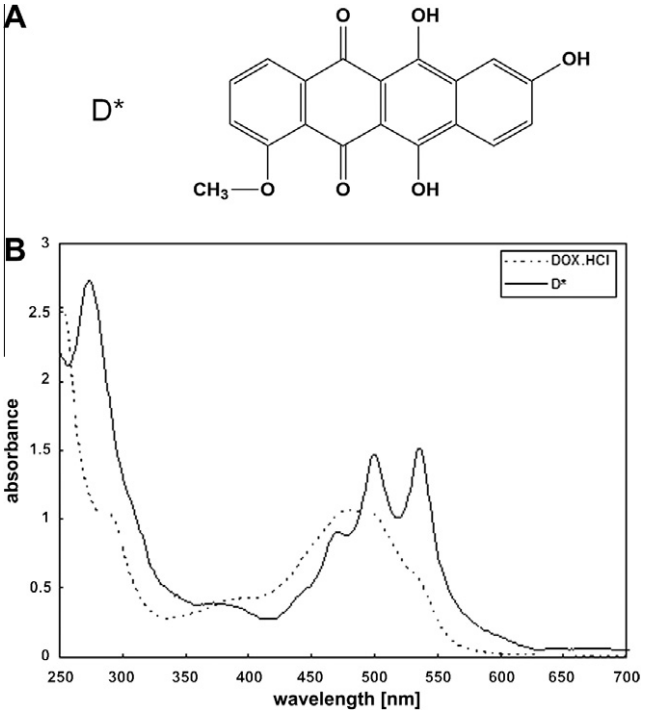

Fig. 1. (A) Structure of 7,8-dehydro-9,10-desacetyldoxorubicinone (D*). (B) Comparison of the UV–VIS spectra of Dox·HCl and D*.

2.2.2. EL-4 mouse T-cell lymphoma

EL-4 cells (ATCC: TIB-181) were grown in cultivation flasks at 37 °C with 5% CO_2 in RPMI 1640 medium (Gibco) without phenol red, supplemented with heat-inactivated 10% v/v fetal calf serum (FCS), 2 mM L-glutamine (Gibco), 50 mM 2-mercaptoethanol (Fluka Chemie, Switzerland), 4.5 g/L glucose, 1.0 mM sodium pyruvate (Sigma–Aldrich), 100 U/mL penicillin, and 100 mg/mL streptomycin.

2.2.3. SW620 human colorectal carcinoma

SW620 (ATCC: CCL-227) cells were grown in cultivation flasks at 37 °C with 5% CO_2 in RPMI 1640 medium (Gibco) without phenol red, supplemented with heat-inactivated 10% v/v fetal calf serum (FCS), 1 mM L-glutamine (Gibco), 50 mM 2-mercaptoethanol (Fluka), 100 U/mL penicillin, and 100 mg/mL streptomycin.

2.3. Cell staining and fluorescence analysis

2.3.1. Spectral unmixing

First, cells were grown in fresh media for 24 h in 24-well plates (NUNC) to adhere to sterile coverslips; then, they were incubated with drug or drug conjugates for 24 or 48 h under the same conditions. Immediately prior to fluorescence detection, samples were washed in PBS/BSA 0.05%.

Visualization and spectral analysis were performed on a Leica TCS SP2 laser scanning confocal microscope equipped with an AOBS (Acousto-Optical Beam Splitter), using 488 nm or 514 nm excitation wavelengths for doxorubicin or D*, 605 nm excitation for Lucifer Yellow, and 633 nm excitation for Dyomics-615. Spectra were measured by spectral scanning technique in the range of 500–700 nm with 10 nm steps.

For unmixing, the reference spectral data of both fluorochromes (doxorubicin and D*) were recorded separately at first step. Such reference spectral λ-stacks were then used to assemble a matrix of fluorochrome-specific weighting factors, which are subsequently applied on spectral λ-stacks of sample containing mixture of both fluorochromes, to determine the contribution of each of them to each image pixel. As a result, we have obtained an image with two separated channels where each of them corresponds to one fluorochrome. Applicability of prepared unmixing matrix was confirmed on spectral λ-stack of cells treated with a mixture doxorubicin and D* for 24 h. Fluorescence and spectra were analyzed using Leica Confocal Software 2.601 build 5137.

Fluorescence Lifetime Imaging (FLIM) was carried on a MicroTime 200 inverted epifluorescence scanning confocal microscope (Picoquant, Germany) [20]. The configuration contained a pulsed diode laser (LDH-P-C-470, 470 nm; Picoquant) providing 80 ps pulses at up to a 40 MHz repetition rate, a proper filter set (Z470/10 (470 nm CWL (Center Wavelength) – the wavelength at the center of the passband and 10 nm FWHM (Full Width at Half Maximum) – the bandwidth at 50% of the maximum transmission) clean-up filter, z470rdc dichroic mirror, and HQ585/70 (585 nm CWL and 70 nm FWHM) band-pass filter) (Chroma Technology, VT, USA), a water immersion objective (1.2 NA, 60×) (Olympus, Japan), and SPAD (Single-Photon Avalanche Diode) detector (MPD, Italy). The FWHM of the overall IRF was 300 ps. Data acquisition was performed in TTTR mode (time-tagged time-resolved), an advanced mode of TCSPC (time-correlated single photon counting). The data were acquired and analyzed in SymphoTime200 software (Picoquant). The FLIM images were analyzed by an amplitude FLIM approach. The TCSPC histogram from the complete image was tail-fitted by the least number of exponentials to obtain satisfactory fit. Up to three components were necessary in the case of polymeric conjugates. The obtained lifetimes were fixed in subsequent fitting of single pixel histograms, by which amplitudes of each component in every pixel of the image were obtained. The average lifetime τ_{AV}

used in histograms and in image creation is an amplitude-weighted average of all components:

$$\tau_{AV} = \frac{\sum_i \tau_i^2 A_i}{\sum_i \tau_i A_i} \quad (1)$$

where τ_I are lifetimes and A_i amplitudes of present components.

2.3.2. Competitive Hoechst staining

Cells (EL-4 T-cell lymphoma) were treated with Dox·HCl or its polymer conjugates in specified concentrations under standard incubation conditions. After 24 h, they were detached with a 0.02% EDTA solution and washed with PBS/BSA 0.05%. Staining with Hoechst 33342 (5 μg/mL; Invitrogen, CA, USA) was performed at 37 °C for 90 min; cells were washed three times with ice-cold PBS/BSA 0.05% and immediately analyzed on a BD LSRII flow cytometer (doxorubicin excitation 488 nm and emission detected via 575BP26 band pass filter (575 nm CWL and 26 nm FWHM), Hoechst 33342 excitation 405 nm and emission detected via 450BP50 (450 nm CWL and 50 nm FWHM) filter (Omega Optical, VT, USA)). Nuclear localization was confirmed on a Compucyte iCys laser Scanning Cytometer (MA, USA) and a Olympus Provis AX-70 fluorescent microscope. Quantitative data were analyzed in three independent experiments. Mean and SD values were obtained using FlowJo software (Tree Star, CA, USA).

3. Results

3.1. Synthesis of monomers, polymer precursors, and conjugates

Monomers, polymer precursors **1**–**3**, polymer conjugates **4**–**6**, and the doxorubicin degradation byproduct 7,8-dehydro-9,10-desacetyldoxorubicinone were synthesized, purified, and characterized by procedures as described in Section 2. Doxorubicin was bound in polymer conjugates via oligopeptide spacers, where the GlyGly spacer is enzymatically nondegradable (conjugate **4**), while the spacer Gly-D,L-PheLeuGly (conjugate **5**) is designed to be degradable by lysosomal enzymes (cathepsin B) enabling thus release of doxorubicin from polymer conjugate. Despite this, it was documented that release of free doxorubicin from polymeric conjugate is not a prerequisite for their efficacy *in vitro* [22].

The HPLC chromatogram of polymer conjugate **4** after purification on a Sephadex LH-20 column in Fig. 2 shows that the polymer conjugate **4** does not contain degradation product D* or free doxorubicin. The same chromatogram was obtained for polymer conjugate **5** after purification.

The HPLC chromatogram of polymer conjugate **5** after incubation in phosphate buffer (pH 7.4 at 37 °C for 0, 5 and 22 h), demonstrating the formation of the degradation byproduct D*, is shown in Fig. 3. Negligible amount of other doxorubicin degradation product with retention time 27.9 min was observed only on the chromatogram with fluorescence detection (Fig. 3b). Other possible doxorubicin-degradable products as 13-dihydrodoxorubicinone, 13-dihydrodoxorubicin, and doxorubicinone were not detected.

3.2. Spectral unmixing

3T3 cells (EL-4, SW620 – not shown) were incubated for 24 h with free doxorubicin hydrochloride and isolated derivative D* in optimal concentration of 0.5 μg/mL or 0.1 μg/mL. Fig. 4A and B show spectra measured by the lambda (spectral) scanning technique in 10 nm steps. The curves obtained served as reference spectra for spectral unmixing [23].

We used these spectra to unmix the control sample, where cells were treated with a mixture of doxorubicin hydrochloride (0.5 μg/mL) + D* (0.1 μg/mL) for 24 h. Separated channels correspond to the reference images and confirm the localization of doxorubicin in nuclei and acidic organelles of cells and the localization of D* fluorescence in the entire cell membrane system (Fig. 5). Results were identical in all tested cancer cell lines.

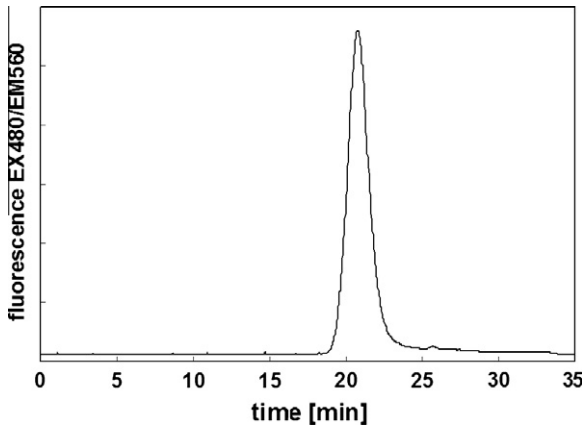

Fig. 2. Polymer conjugate **4** after purification on a Sephadex LH-20 column in methanol. Record from the fluorescence detector with Ex = 480 nm and Em = 560 nm.

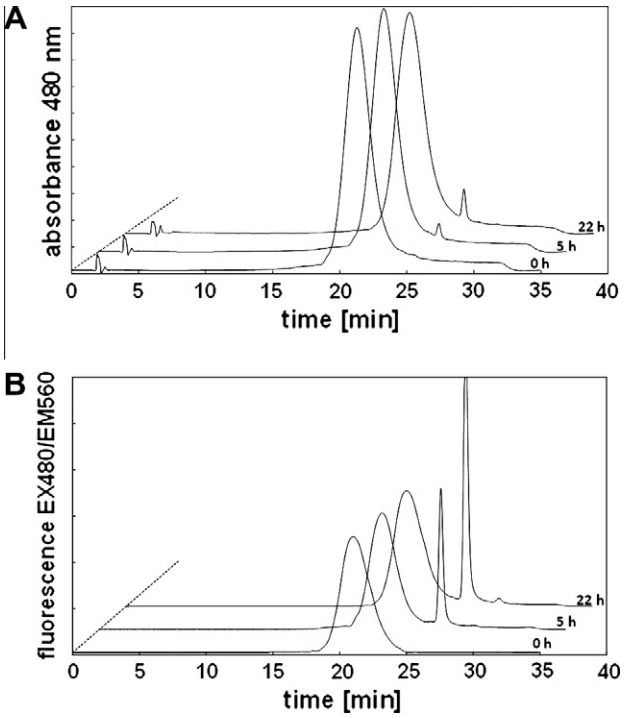

Fig. 3. HPLC chromatogram of polymer conjugate **5** incubated in a phosphate buffer, pH 7.4, at 37 °C for 0, 5 and 22 h. (a) Record from the UV–VIS detector at 480 nm; (b) record from the fluorescence detector with Ex = 480 nm and Em = 560 nm.

3.3. Conjugate spectral analysis

3T3, EL-4, SW620 cells were incubated for 24 or 48 h with Dox-polymer conjugate **5** (structure corresponding to PK1) in optimal doxorubicin concentration of 10 μg/mL. Polymer conjugate **5** was either added directly to the cell culture or left in cell-free medium for the same incubation time (24 or 48 h) and under the same incubation conditions: 37 °C, 5% CO_2. Then, just before visualization, the polymer conjugate **5** solution in

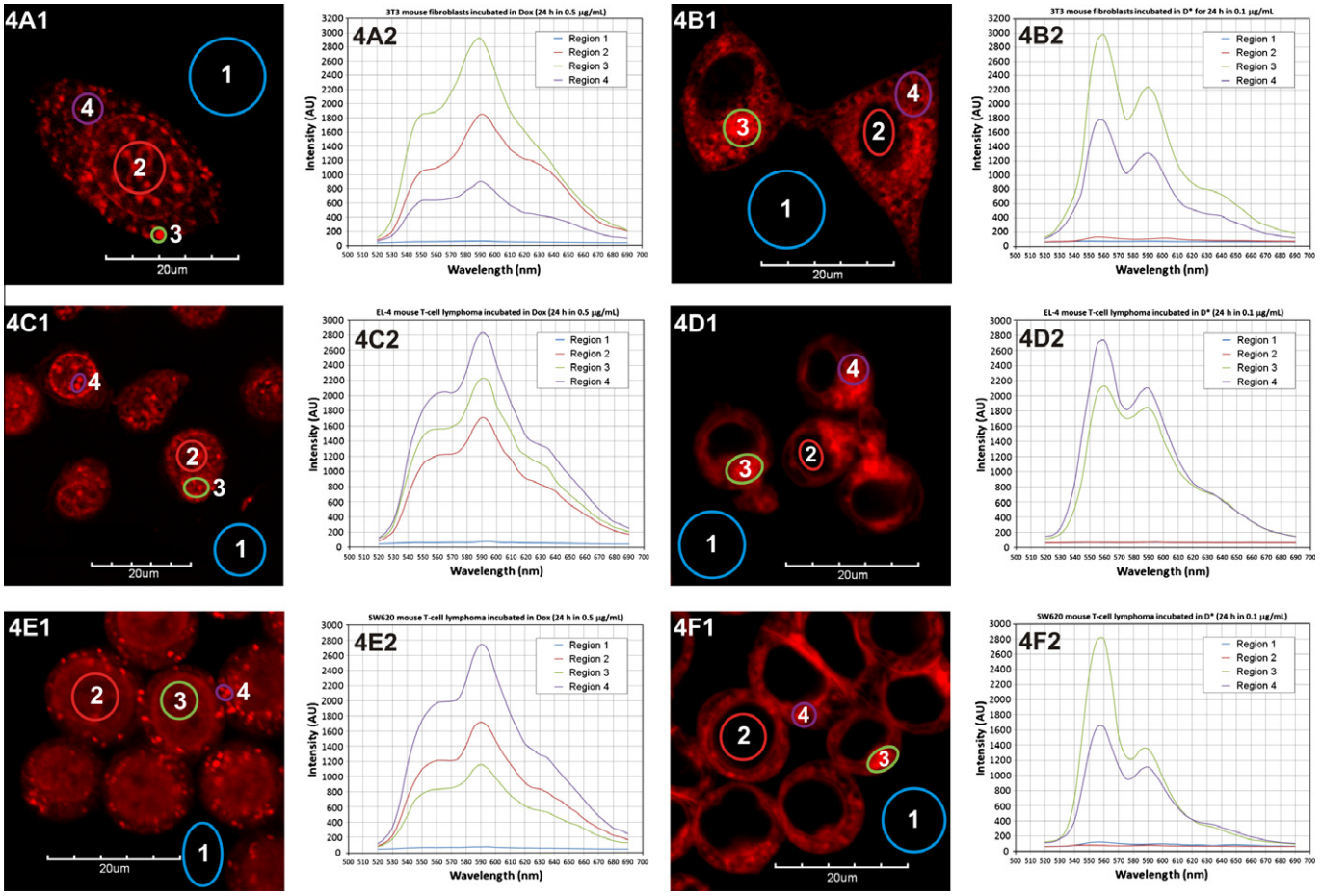

Fig. 4. 3T3 mouse fibroblasts (A and B), EL-4 mouse T-cell lymphoma (C and D), and SW620 human colorectal carcinoma (E and F) were incubated for 24 h with either free doxorubicin hydrochloride 0.5 μg/mL (A, C, and E) or with free D* 0.1 μg/mL (B, D, and F). Spectra were measured on a Leica SP2 confocal microscope with 488 nm excitation by a lambda scanning module in 10-nm steps. Areas where spectral properties were analyzed were selected inside, as well as outside the nucleus, in areas with different intensity; the blue circle represents the background. Obtained spectral profiles are on right panel of every image, designed as No. **2**.

cell-free medium was added for 3 h incubation to the fresh cell culture. Obtained spectra (excitation 488 nm) are shown in Fig. 6, where Fig. 6A represents spectra after 24 h incubation with cells, Fig. 6B represents spectra after 48 h incubation with cells, and Fig. 6C represents spectra of conjugate **5** incubated for 45 h in media without the cells plus 3 h incubation with cells. According to Fiallo et al. [13], we have analyzed the 560/590 index (for excitation 488 or 514 nm), which enables the differentiation between D* and Dox fluorescence, see Table 2.

From the obtained spectral profiles, and similarly, from the 560/590 index, the increase in maxima at 560 nm is clearly visible, confirming the time-dependent increase in proportion of the degradation byproduct D*. Even after 24 h of incubation, the spectral profile and 560/590 index much more resemble that of D* than Dox. This means that even after 24 h incubation, D* emission almost completely superimposed the emission of Dox; the majority of signals originate from the degradation byproduct localized in cellular membranes; and the real signal of doxorubicin bound to the polymeric carrier could be detectable only after unmixing the individual signals.

The spectral profile in Fig. 6C is identical to that of Fig. 6B, proving that the formation of D* from polymer conjugate **5** is a spontaneous phenomenon and not a metabolic degradation stage.

3.4. Intracellular localization of polymeric conjugates

The spectral unmixing technique allows us to distinguish the fluorescence of Dox bound to a polymeric carrier from the much stronger fluorescence of the free degradation byproduct D*. Fig. 7 shows unmixed images of 3T3 fibrosarcoma incubated with polymer conjugate **5** for 48 h, exhibiting an accumulation of D* in the entire cell membrane system, while fluorescence of Dox is primary accumulated in endosome-like spots, although minimal fluorescence from membranes is also detectable.

To confirm intracellular localization of the conjugate, we have used polymer conjugate **6** co-stained with a second Dyomycs-615 fluorescent probe, which has minimal spectral crosstalk with Dox. Endosomes inside cells were counterstained with a dextran-Lucifer Yellow probe (Invitrogen). One hundred percent co-localization of the unmixed Dox signal with Dyomycs-615 fluorochrome was detected, and both these colors were co-localized with the dextran-LY endosomal probe as documented in Fig. 8 on the right bottom merged component image. Fig. 8 proves the primary accumulation of such polymeric conjugates occurring in the endocytic compartment; but a much weaker signal of Dox/Dy-615 was also documented from other cellular membranes, as we have documented before [21].

3.5. Fluorescence lifetime imaging

3T3 cells were incubated for 24 h in optimal concentration of free doxorubicin hydrochloride (1.0 μg/mL), isolated derivative D* (0.1 μg/mL), or polymer conjugates **4** and **5** (10 μg/mL). We analyzed the fluorescence lifetime of doxorubicin, D*, and polymeric conjugates **4** and **5**, both in solution of media to obtain average lifetime (aLT) for all tested components and also inside cells after 24 h

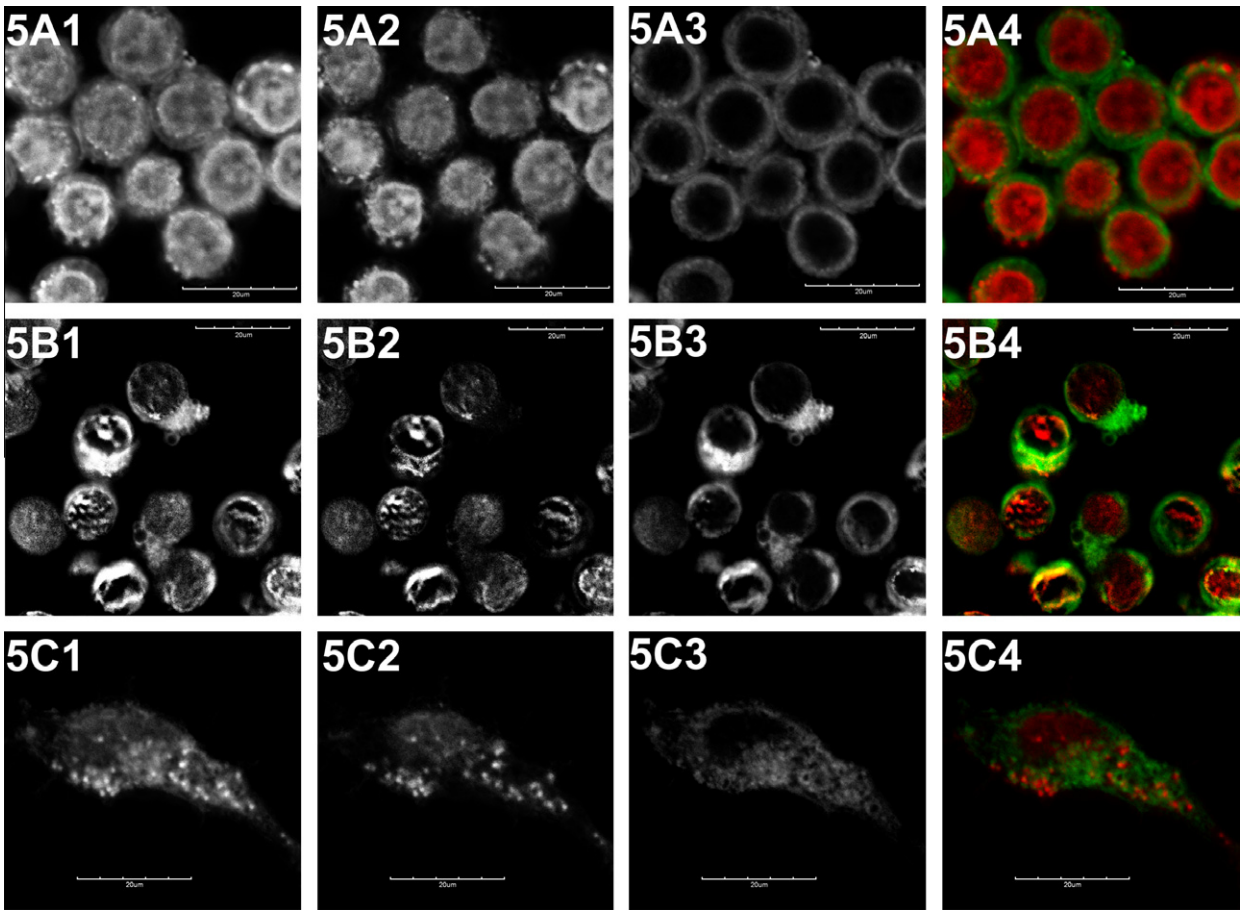

Fig. 5. 3T3 mouse fibroblasts (A), EL-4 mouse T-cell lymphoma (B), and SW620 human colorectal carcinoma (C) were incubated for 24 h with mixture of free doxorubicin hydrochloride (0.5 μg/mL) and D* (0.1 μg/mL) for 24 h. Spectra were measured on a Leica SP2 confocal microscope with 488 nm excitation by a lambda scanning module in 10-nm steps. Spectral unmixing was performed by the standard Leica unmixing algorithm included in the software package, based on reference spectra obtained in the previous step. Every image consists of four panels, where panel **1** represents image as average projection of whole obtained spectral stack, panel **2** represents intracellular localization of doxorubicin after spectral unmixing, similarly panel **3** represents intracellular accumulation of D*, and panel **4** represents merged channels in false colors, where doxorubicin is in red and D* is in green.

treatment. Values are summarized in Table 3. The detected increase in aLT in the cellular model is caused by background cellular autofluorescence.

Fig. 9A and B show lifetime distributions of tested drugs and conjugates and their intracellular locations. From the measured lifetime distribution, it is clear that D* is present in both tested systems. Free doxorubicin, unlike the polymer-bound drug, is accumulated in nuclear DNA and inside the lumen of endosomes and lysosomes [21], being the only cellular locations without a detectable amount of D*. All other compartments are occupied with a mixture of Dox and D*, which is detectable as a second peak at approx. 3 ns in the lifetime distribution. Free D* is accumulated in the entire cell membrane system, as it has been postulated before [13]. In the experiment, where cells were incubated with the mixture of Dox and D*, we were able to detect two peaks – first at 1.5 ns, corresponding to the fluorescence lifetime of free Dox; and a second peak at about 3 ns, corresponding to a mixture of both components. Intracellular lifetime distribution also corresponds to previous samples with separated drugs.

We were not able to detect any trace of free Dox in any of the tested polymer conjugates at its lifetime peak of 1.5 ns. Only in the case of polymer conjugate **5** after 24 h of incubation, were we able to detect a minor lifetime peak at approx 2.5 ns, which corresponds to the conjugate accumulated in endosomes and lysosomes, but with D* contamination prolonging the lifetime. Such peaks after 48 h of incubation disappear (not shown), indicating the continuous decomposition of the conjugate and an increased concentration of D*, which at that time completely overlaps Dox fluorescence.

3.6. Indirect detection of doxorubicin in nuclei

EL-4 cells incubated for 24 h (37 °C, 5% CO_2) with free Dox·HCl or with Dox-polymer conjugates **4** (not shown) and **5** were then stained with Hoechst 33342 and analyzed by flow cytometry. Fig. 10 shows that the fluorescence of Hoechst 33342 decreases depending on the increased concentration of free Dox, while an increased concentration of polymeric conjugate **5** (which does not release Dox in the *in vitro* system [22]) has no effect on Dox nuclear accumulation.

4. Discussion

Water-soluble polymer conjugates of Dox **4**–**6** based on *N*-(2-hydroxypropyl)methacrylamide copolymers were synthesized and characterized. The Dox degradation byproduct 7,8-dehydro-9,10-desacetyldoxorubicinone (D*) (Fig. 1) was isolated from a solution of polymeric conjugate **5** in a phosphate buffer and characterized by HPLC, MS (NALDI), and UV/VIS spectrometry.

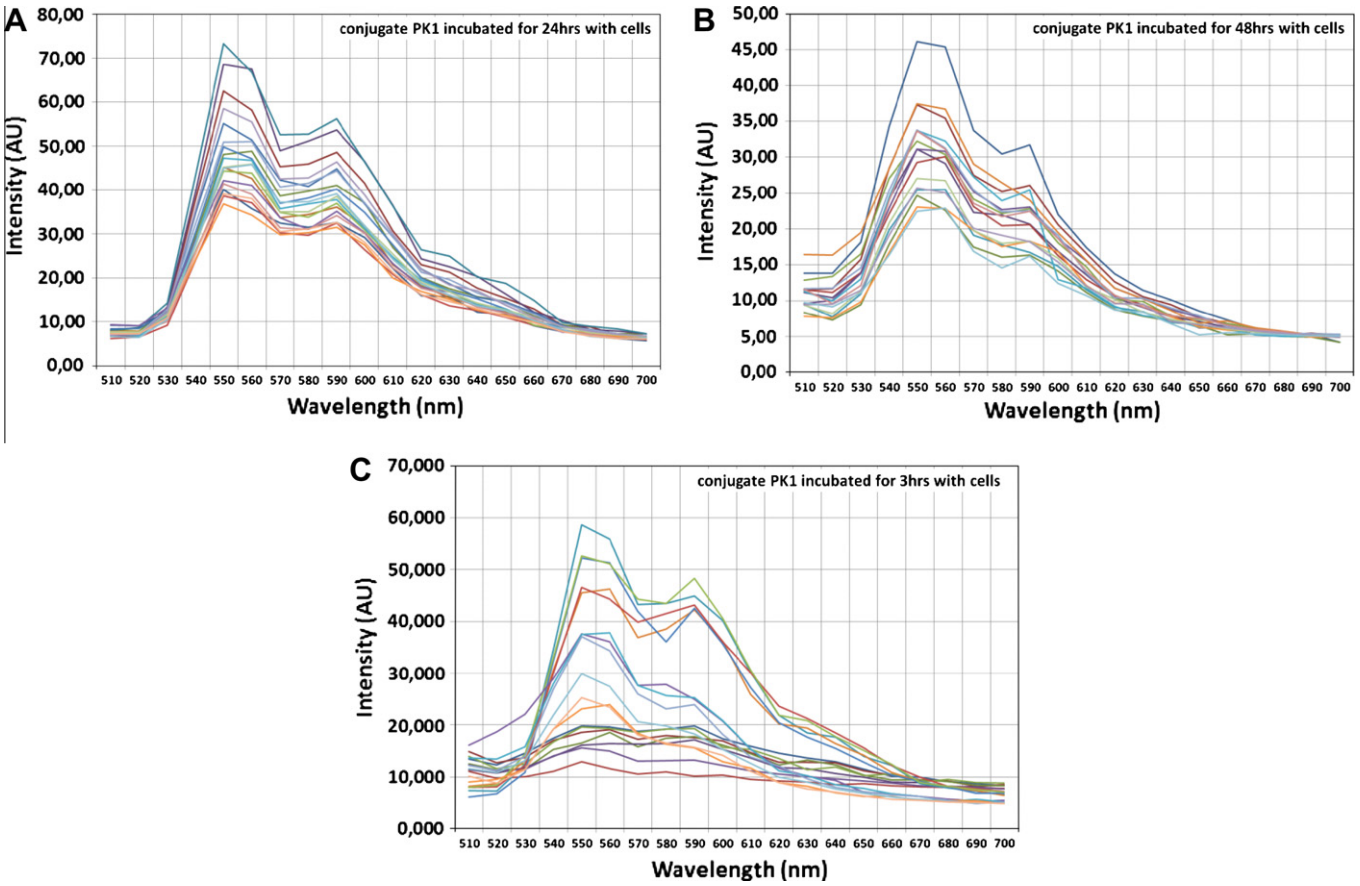

Fig. 6. Spectral analysis of 3T3 cells incubated with conjugate **5** in 10 μg/mL concentration for 24 h (A), 48 h (B). Spectral profiles were obtained from 19 regions of interest randomly placed inside bright as well as dim compartments of cell. (C) Spectra of conjugate **5**, which was left in cell-free medium for 45 h under the same incubation conditions (37 °C, 5% CO_2) and added for 3 h of incubation to the fresh cell culture. Spectra were measured on a Leica SP2 confocal microscope with 488 nm excitation by a lambda scanning module in 10-nm steps.

Table 2
560/590 index spectral curves of tested drugs and polymeric conjugates. Each index was calculated as an average of at least 25 spectral profiles (from areas inside cells with both intensive and dim signal) obtained from five different cells located at three independent slides.

Sample		Excitation	560 nm	590 nm	560/590 index	SD	
Doxorubicin		488	43	62	**0.693**	0.021	
		514	33	42	**0.785**	0.034	
D*		488	83	65	**1.277**	0.065	
		514	103	80	**1.285**	0.037	
Conjugate **5** (PK1)	24 h	488	37	27	**1.371**	0.039	]*
	48 h		47	41	**1.146**	0.078	
	48 + 3 h		64	50	**1.280**	0.083	

* Represents statistical significance at $P < 0.0003$.

The direct detection of Dox uptake and intracellular localization based on fluorescent techniques could be problematic due to Dox degradation in aqueous solutions, resulting in the formation of 7,8-dehydro-9,10-desacetyldoxorubicinone (D*) [13]. All currently published results, based on techniques utilizing Dox fluorescence, include partially false positivity originating from a certain amount of D* present in all Dox samples incubated in aqueous buffer media. Significant complications or even incorrect interpretation of these obtained data can rise from the fact that this degradation byproduct originates in the aqueous solution spontaneously, not only from free Dox, but also from some Dox-containing polymer conjugates. The quantum yield of D* fluorescence is so high, that it is able to completely overshadow the fluorescence of Dox. This was the reason why we had to use an "optimal concentration" (varying for different drugs or conjugates by two orders of magnitude), allowing us to detect and isolate the much lower true Dox signal.

To separate these overlapping signals, we had to use either a spectral unmixing technique or fluorescence lifetime analysis. Spectral analysis allowed us to separate fluorescent signals, but because of a large disproportion of D* and Dox quantum yield, unmixing in areas with a weak Dox signal was still disputable. Spectral unmixing was successful in the case of the Dox and D* mixture (1:5). In case of polymer conjugate **5**, the obtained image was very dim, and both signals were still presented together in the majority of cellular compartments, only with different intensities. The enhanced accumulation of polymer conjugate **5** in the endosomal compartment was confirmed by co-localization with a dextran-Lucifer Yellow probe.

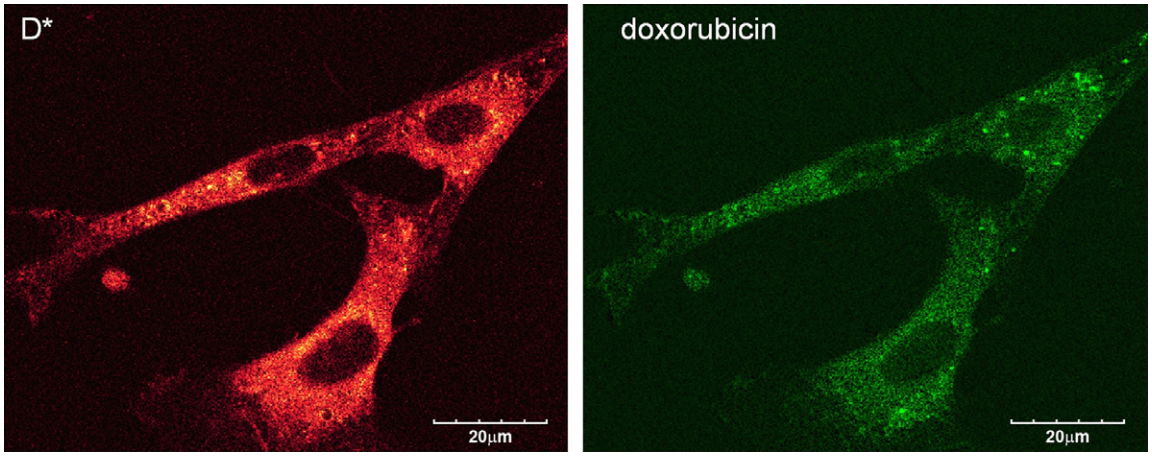

Fig. 7. Spectral unmixing of 3T3 cells incubated with conjugate **5** for 48 h. Spectra were measured on a Leica SP2 confocal microscope with 488 nm excitation by a lambda scanning module in 10-nm steps. Spectral unmixing was performed by the standard Leica unmixing algorithm included in the software package, based on reference spectra obtained in the previous step.

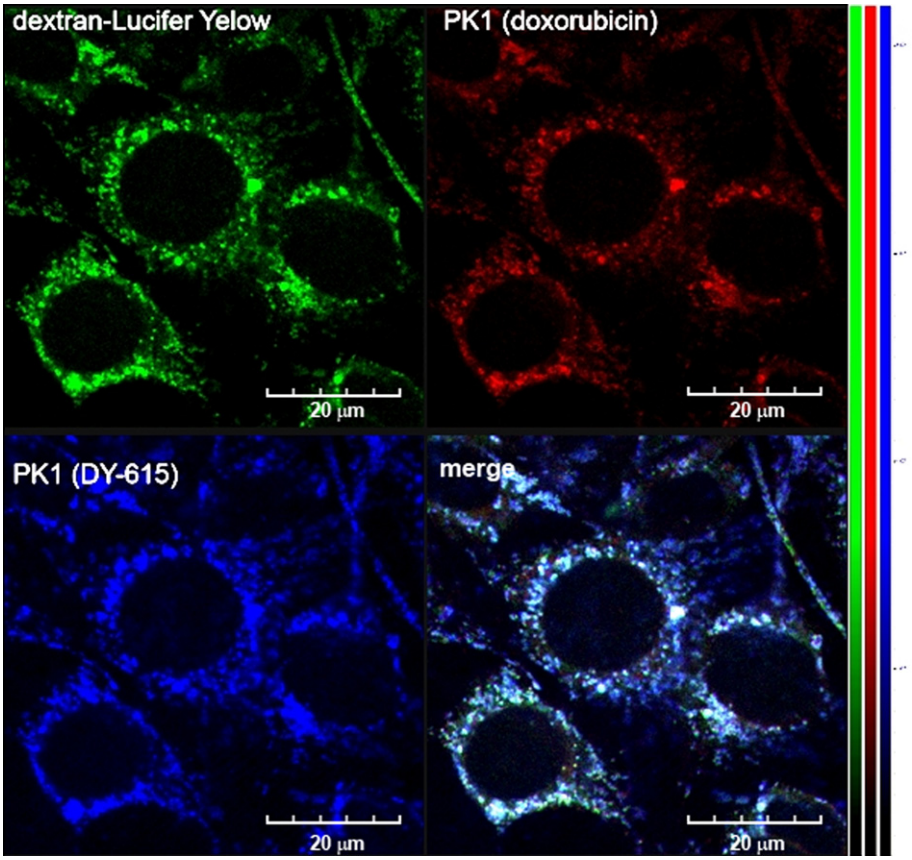

Fig. 8. Intracellular localization of polymer conjugate **6** (identical to conjugate **5**, but co-stained with a Dyomycs-615 fluorescent probe; Ex 633 nm, Em 670–750 nm) inside 3T3 cells after 48-h treatment. The endosomes inside the cell were counterstained with a dextran-Lucifer Yellow probe (Ex 405 nm, Em 500–600 nm). The fluorescence of Dox and D* (Ex 488 nm, Em 520–650 nm) was separated by the standard Leica unmixing algorithm included in the software package, based on the reference spectra described above and only that of doxorubicin is shown. The image on the right bottom is a merged image of previously described channels to confirm co-localization of doxorubicin and Dy-615 probe labeling polymeric carrier with endosomal compartment labeled by dextran-Lucifer Yellow probe.

On the other hand, fluorescence lifetime analysis was not (owing to the huge difference in the lifetime of Dox (1.5 ns) and D* (4.6 ns)) influenced by fluorescent intensity, and unmixing of both signals was much more precise. From distribution histograms shown in Fig. 9A and images in Fig. 9B, it was clear that in the cells incubated with the free drug, Dox was located inside nuclear DNA and inside endosomes/lysosomes as previously documented [21], and the detectable intracellular localization of D* was limited to the entire cellular membrane system without any signal from the nucleus. This difference in localization of Dox and D* can be explained by the different hydrophobicity of Dox (containing aminosaccharide daunosamine in its structure) and the highly hydrophobic D* (no saccharides or amino groups in the molecule). Even after incubation with free Dox (Dox·HCl), there was a very

Table 3
Excited state fluorescence lifetimes of tested drugs and conjugates in cell-free and cellular system.

Conjugate	Doxorubicin	D*	Conjugate **4** (GG)	Conjugate **5** (GFLG)
Excited state fluorescence lifetimes (ns) – cell-free system	1.1	3.9	1.2/4.2*	1.2/4.1*
Excited state fluorescence lifetimes (ns) – cellular system	1.5	4.1	2.3/4.5*	2.3/4.4*

* However, for the conjugates, three components were necessary to satisfactorily fit the measured decay; presented are those with significant amplitudes. Amplitude of the third component was imponderable.

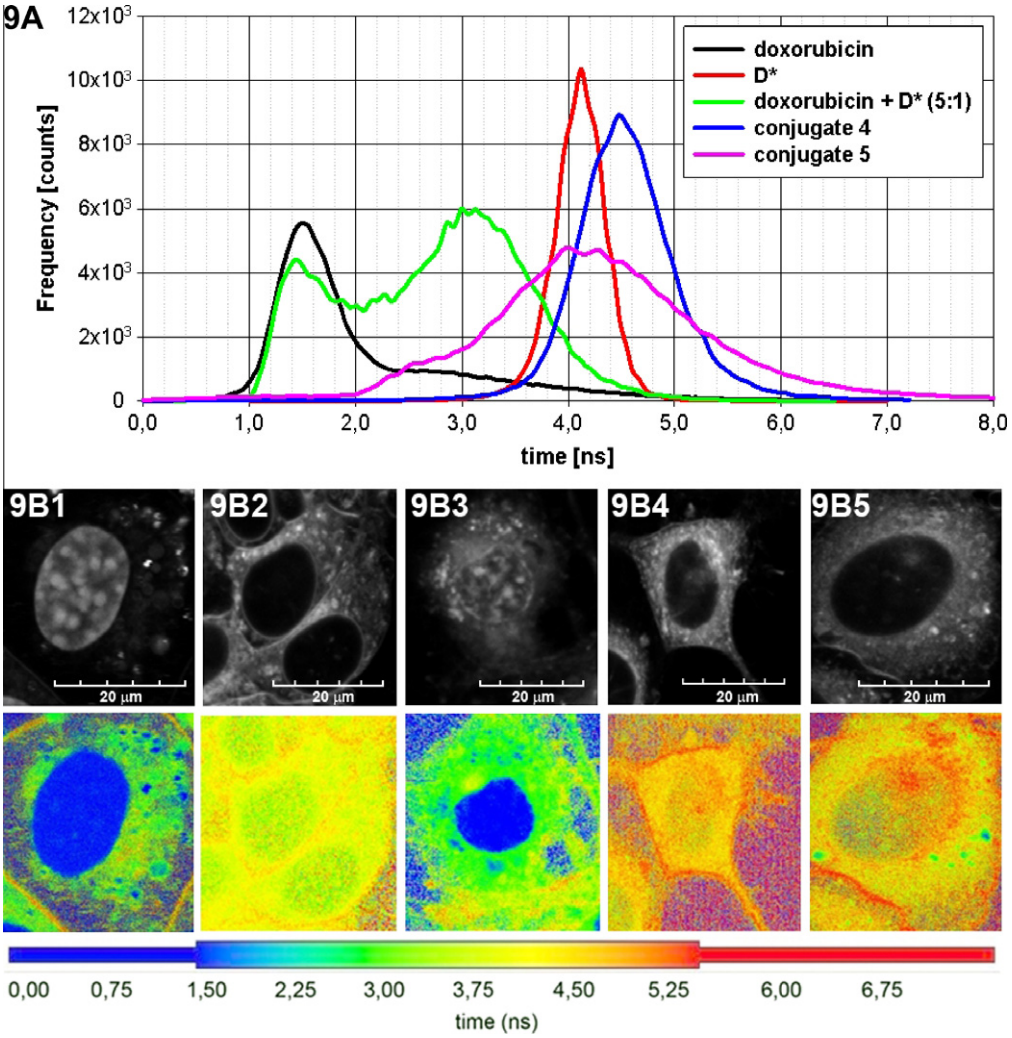

Fig. 9. Fluorescence lifetime imaging. (A) The intensity-weighted average lifetime distributions of the tested drugs and conjugates as quantified by SymphoTime software (PicoQuant). In (B), there are shown the fluorescent images (top panel) and FLIM images (without the intensity component) in false colors (bottom panel), based on the lifetime distribution as analyzed in (A). (B1) Doxorubicin; (B2) D*; (B3) doxorubicin + D* (5:1); (B4) conjugate **4**, (B5) conjugate **5**.

weakly detectable signal from other cellular membranes, which represents a mixture of Dox and D* signals with a lifetime of about 3 ns. This confirms the statement of Fiallo et al. [13] that D* originates spontaneously in aqueous media from the parent drug. Identical results, but with much more precise distribution, were documented in cells treated with a mixture of Dox and D*. While the nucleus and endosomes/lysosomes record lifetime signals corresponding to free Dox (D* probably cannot cross nucleus membranes), cellular membrane systems were again loaded with a mixture of both drugs, with a lifetime of about 3 ns. It was not possible to detect any area loaded with a separated D* lifetime signal (4.5 ns). It seems that both molecules were accumulated in the lipophilic membrane environment in similar amounts due to the hydrophobic interaction of similar aglycon parts of their molecules. There was clear co-localization of both signals from the same cellular membranes, with a typical 3 ns lifetime signal.

Although the lifetimes of both polymeric conjugates (polymer-bound Dox) in solution were about 2.5 ns, the major signal obtained *in vitro* has a lifetime of about 4.5 ns, corresponding to the lifetime of D*. We were unable to detect any lifetime signal corresponding to free Dox up to 48 h of incubation in any of the tested cases, and we can confirm our previous statement that such polymer conjugates do not release free doxorubicin in the *in vitro* system [21,22]. Moreover, the intracellular accumulation of the polymer conjugate with bound doxorubicin (lifetime 2.5 ns) in the endosomal compartment was documented only with conjugate **5**, but never detected with conjugate **4**. Also, lifetime distribution in the case of conjugate **5** (maximum at about 4.2 ns) was broadly

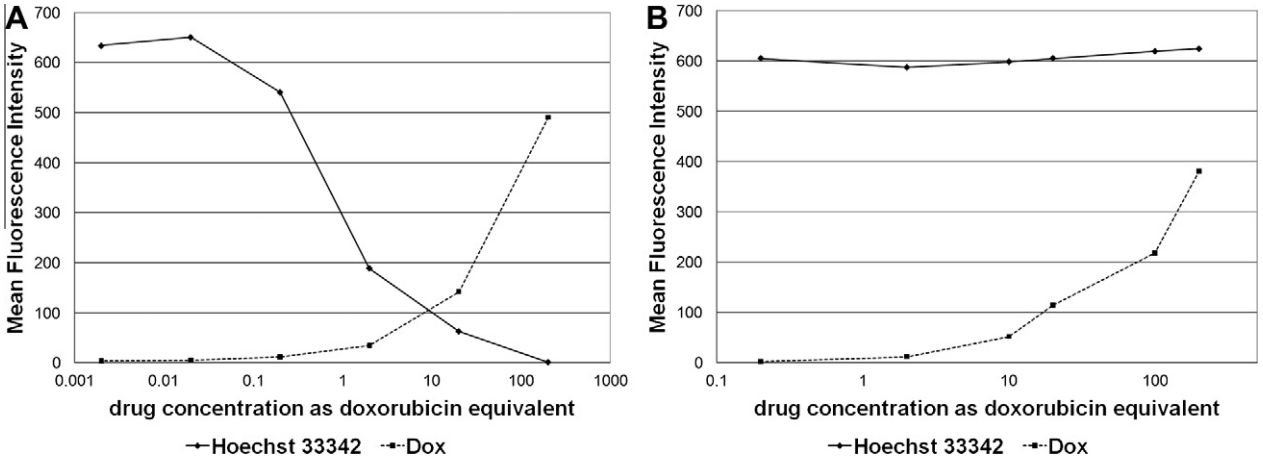

Fig. 10. In (A) is shown the analysis of decreased Hoechst 33342 accumulation inside the nuclei of EL-4 cells, after treatment with free doxorubicin, as a result of intercalating competition. In (B) is shown no detectable decrease in Hoechst staining; however, cells are highly loaded with polymer conjugate **5**, bearing doxorubicin.

spread to shorter lifetimes (about 3 ns), which corresponds to the co-localization of the polymer-bound form of Dox with D* in the cellular membrane system, as documented earlier [21]. Lifetime distribution of conjugate **4** almost corresponded to the distribution of D*, and there was no detectable trace of a Dox signal (neither free nor polymer-bound). The data confirm our former statement [21,22] that polymer conjugates bearing Dox bound to a polymer backbone, via a less hydrophobic GlyGly spacer, are accumulated with much lower intensity in lipophilic portions of the cell membrane than conjugates containing the more lipophilic Gly-D,L-Phe-LeuGly spacer.

To analyze the nuclear accumulation of free Dox (Dox·HCl) or Dox released from different drug delivery systems by flow cytometry is problematic, not only because of the D* spectral overlap, but also due to the accumulation of the free drug in other cellular compartments, such as endosomes and lysosomes. Because the major cytotoxic effect of free Dox is targeted against nuclear DNA (although the effect on mitochondrial metabolism and plasma membrane integrity was also documented [24]), we could advantageously use, in lieu of direct Dox fluorescence quantification, an indirect analysis based on the competitive intercalation of Dox with Hoechst 33342 into nuclear DNA. Hoechst 33342 is a commonly used fluorescent probe with well-characterized spectral properties, which increases its fluorescence activity upon DNA intercalation. Thus, the decrease in Hoechst staining could be even more sensitive than the increase in Dox fluorescence; furthermore, there is no doubt about the nuclear localization of this known probe.

5. Conclusions

The fluorescence of doxorubicin can be substantially overlapped with its degradation byproduct D*. Spectral unmixing or FLIM analysis is the only methods to separate true signals originating from free doxorubicin, polymer-bound doxorubicin, and D* or eventually Dox/D* complexes. Using these techniques, we have confirmed our former observation concerning the intracellular localization of some HPMA-based polymer conjugates. Indirect detection of doxorubicin nuclear accumulation, based on the competitive intercalation with Hoechst 33342, is a very sensitive technique and is able to eliminate any inaccuracy caused by endosomal/lysosomal accumulation of the drug or by D* spectral overlap.

Acknowledgments

This research was supported by the Grant Agency of the Academy of Sciences of the Czech Republic (GAAV) Grant Nos. IAA400200702 and IAAX00500803, by the Institutional Research Concept AV OZ 502 00510, and by the Ministry of Education of the Czech Republic Grant LC06063.

References

[1] M.C. Perry, The Chemotherapy Source Book, Lippincott Williams & Wilkins, Philadelphia, 2007.
[2] A.L. Ferreira, L.S. Matsubara, B.B. Matsubara, Anthracycline-induced cardiotoxicity, Cardiovasc. Hematol. Agents Med. Chem. 6 (2008) 278–281.
[3] R. Duncan, Designing polymer conjugates as lysosomotropic nanomedicines, Biochem. Soc. Trans. 35 (2007) 56–60.
[4] B. Rihova, O. Hovorka, L. Kovar, M. Kovar, T. Mrkvan, M. Sirova, K. Ulbrich, HPMA–anticancer drug conjugates, in: L.H. Reddy, P. Couvreur (Eds.), Macromolecular Anticancer Therapeutics, Springer Science + Bussiness Media, New York, 2010, pp. 87–132.
[5] A. Samad, Y. Sultana, M. Aqil, Liposomal drug delivery systems: an update review, Curr. Drug Deliv. 4 (2007) 297–305.
[6] T. Lammers, W.E. Hennink, G. Storm, Tumour-targeted nanomedicines: principles and practice, Br. J. Cancer 99 (2008) 392–397.
[7] Y. Matsumura, K. Kataoka, Preclinical and clinical studies of anticancer agent-incorporating polymer micelles, Cancer Sci. 100 (2009) 572–579.
[8] H.K. Sajja, M.P. East, H. Mao, Y.A. Wang, S. Nie, L. Yang, Development of multifunctional nanoparticles for targeted drug delivery and noninvasive imaging of therapeutic effect, Curr. Drug Discov. Technol. 6 (2009) 43–51.
[9] R.M. Schiffelers, G. Storm, Liposomal nanomedicines as anticancer therapeutics: beyond targeting tumor cells, Int. J. Pharm. 364 (2008) 258–264.
[10] I.J. Majoros, C.R. Williams, J.R. Baker Jr., Current dendrimer applications in cancer diagnosis and therapy, Curr. Top. Med. Chem. 8 (2008) 1165–1179.
[11] L.W. Seymour, D.R. Ferry, D.J. Kerr, D. Rea, M. Whitlock, R. Poyner, C. Boivin, S. Hesslewood, C. Twelves, R. Blackie, A. Schatzlein, D. Jodrell, D. Bissett, H. Calvert, M. Lind, A. Robbins, S. Burtles, R. Duncan, J. Cassidy, Phase II studies of polymer-doxorubicin (PK1, FCE28068) in the treatment of breast, lung and colorectal cancer, Int. J. Oncol. 34 (2009) 1629–1636.
[12] B. Rihova, Clinical experience with anthracycline antibiotics–HPMA copolymer–human immunoglobulin conjugates, Adv. Drug Deliv. Rev. 61 (2009) 1149–1158.
[13] M. Fiallo, A. Laigle, M.N. Borrel, A. Garnier-Suillerot, Accumulation of degradation products of doxorubicin and pirarubicin formed in cell culture medium within sensitive and resistant cells, Biochem. Pharmacol. 45 (1993) 659–665.
[14] K.K. Karukstis, E.H. Thompson, J.A. Whiles, R.J. Rosenfeld, Deciphering the fluorescence signature of daunomycin and doxorubicin, Biophys. Chem. 73 (1998) 249–263.
[15] K. Ulbrich, V. Subr, J. Strohalm, D. Plocova, M. Jelinkova, B. Rihova, Polymeric drugs based on conjugates of synthetic and natural macromolecules. I. Synthesis and physico-chemical characterisation, J. Control Release 64 (2000) 63–79.
[16] J. Drobnik, J. Kopecek, J. Labsky, P. Rejmanova, J. Exner, V. Saudek, J. Kalal, Enzymatic cleavage of side chains of synthetic water-soluble polymers, Makromol. Chem. 177 (1976) 2833–2848.
[17] B. Rihova, M. Bilej, V. Vetvicka, K. Ulbrich, J. Strohalm, J. Kopecek, R. Duncan, Biocompatibility of *N*-(2-hydroxypropyl) methacrylamide copolymers

containing adriamycin. Immunogenicity, and effect on haematopoietic stem cells in bone marrow in vivo and mouse splenocytes and human peripheral blood lymphocytes in vitro, Biomaterials 10 (1989) 335–342.
[18] V. Subr, K. Ulbrich, Synthesis and properties of new *N*-(2-hydroxypropyl)methacrylamide copolymers containing thiazolidine-2-thione reactive groups, React. Funct. Polym. 66 (2006) 1525–1538.
[19] J. Strohalm, J. Kopecek, Poly[N-(2-hydroxypropyl)methacrylamide]. IV. Heterogeneous polymerization, Angew. Makromol. Chem. 70 (1978) 109–118.
[20] M. Wahl, F. Koberling, M. Patting, H. Rahn, R. Erdmann, Time-resolved confocal fluorescence imaging and spectroscopy system with single molecule sensitivity and sub-micrometer resolution, Curr. Pharm. Biotechnol. 5 (2004) 299–308.
[21] O. Hovorka, T. Etrych, V. Subr, J. Strohalm, K. Ulbrich, B. Rihova, HPMA based macromolecular therapeutics: internalization, intracellular pathway and cell death depend on the character of covalent bond between the drug and the peptidic spacer and also on spacer composition, J. Drug Target 14 (2006) 391–403.
[22] B. Rihova, J. Strohalm, O. Hovorka, V. Subr, T. Etrych, P. Chytil, R. Pola, D. Plocova, J. Boucek, K. Ulbrich, Doxorubicin release is not a prerequisite for the in vitro cytotoxicity of HPMA-based pharmaceuticals: in vitro effect of extra drug-free GlyPheLeuGly sequences, J. Control Release 127 (2008) 110–120.
[23] T. Zimmermann, Spectral imaging and linear unmixing in light microscopy, Adv. Biochem. Eng. Biotechnol. 95: (2005) 245–265.
[24] M. Binaschi, M. Bigioni, A. Cipollone, C. Rossi, C. Goso, C.A. Maggi, G. Capranico, F. Animati, Anthracyclines: selected new developments, Curr. Med. Chem. 1 (2001) 113–130.